The predominant pathway for "early" vision

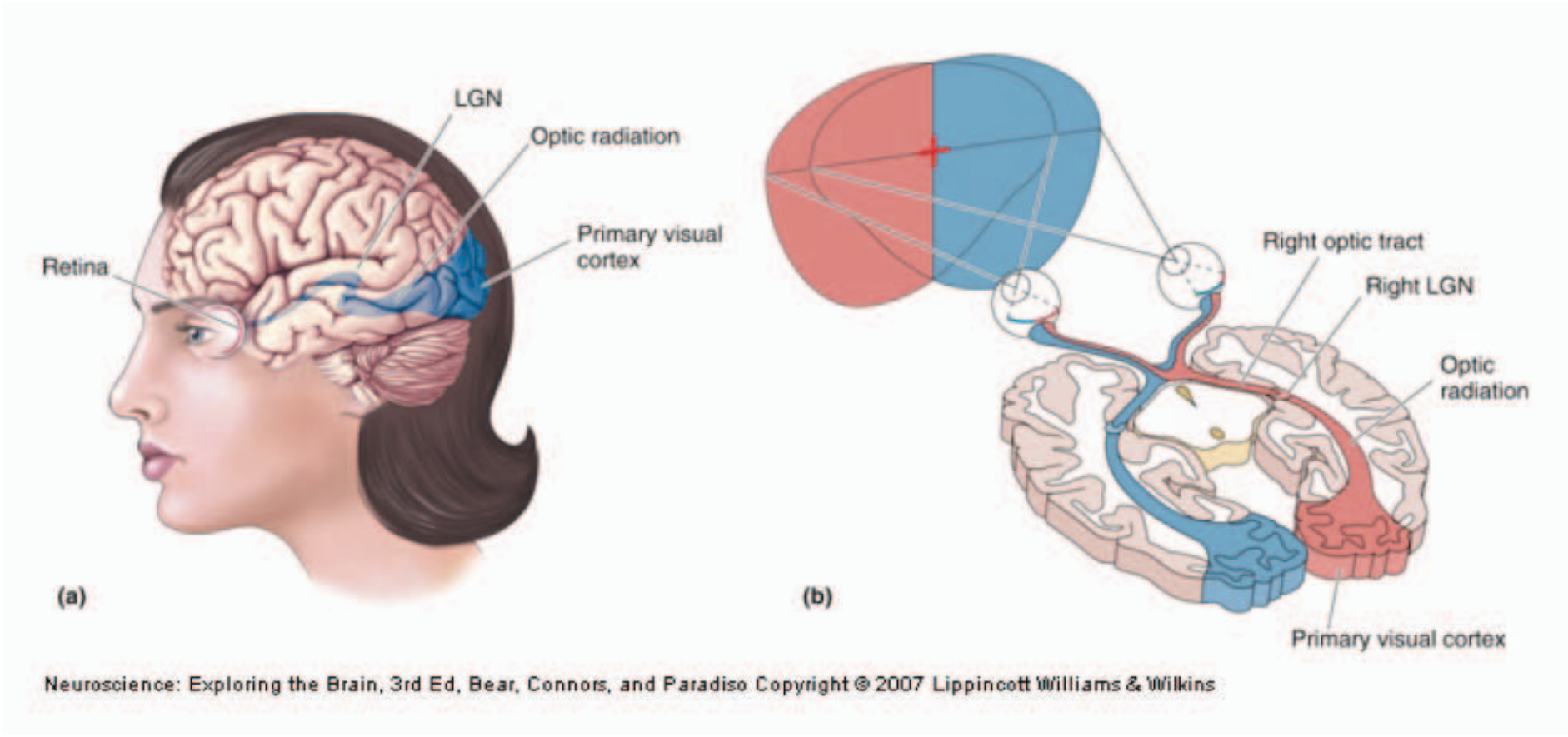

Vision starts in the eye - and is largely mapped 1:1 across space (retinotopy)

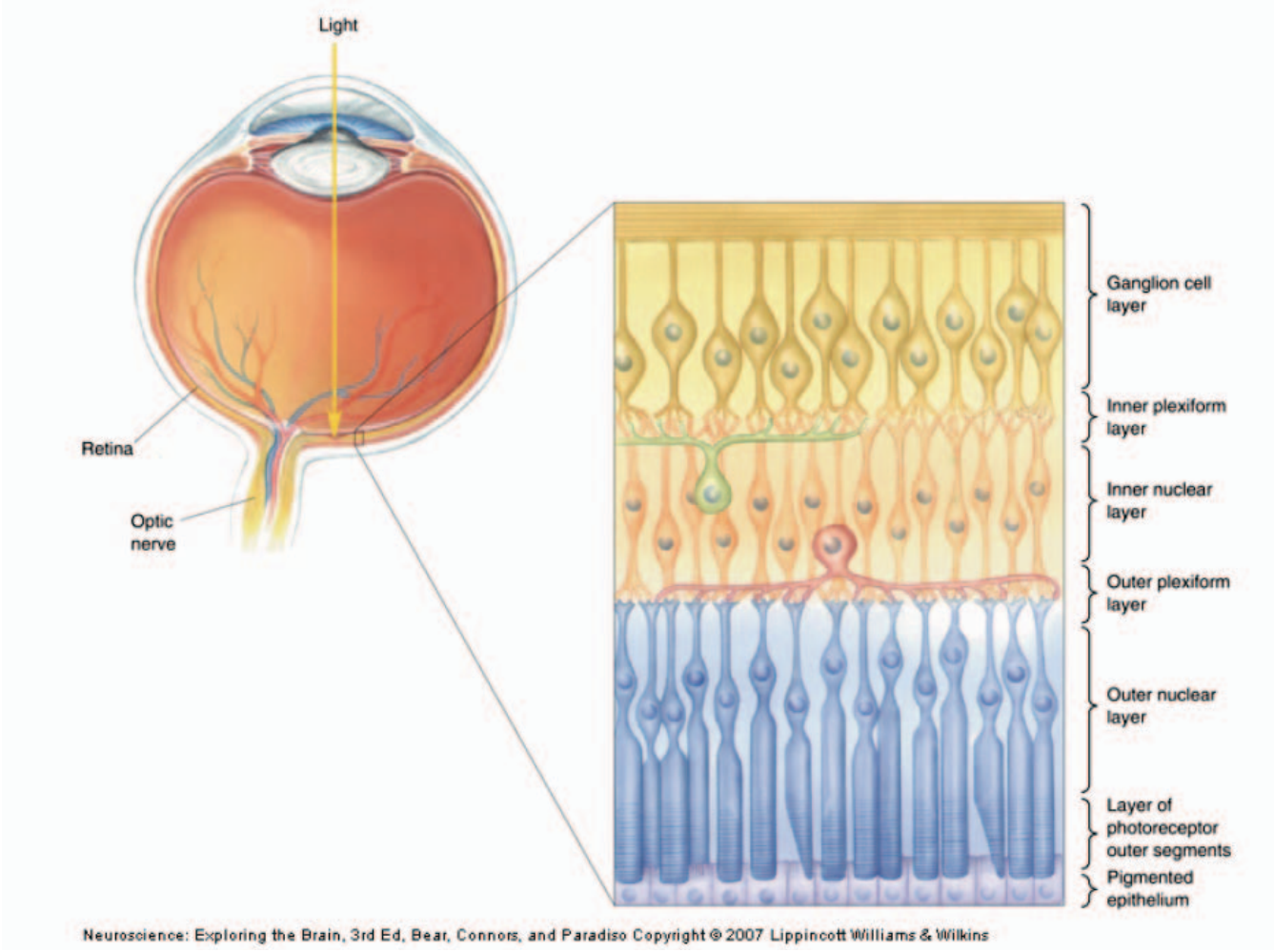

Many output cells from the retina, i.e., retinal ganglion cells, have a ∇^2 receptive field

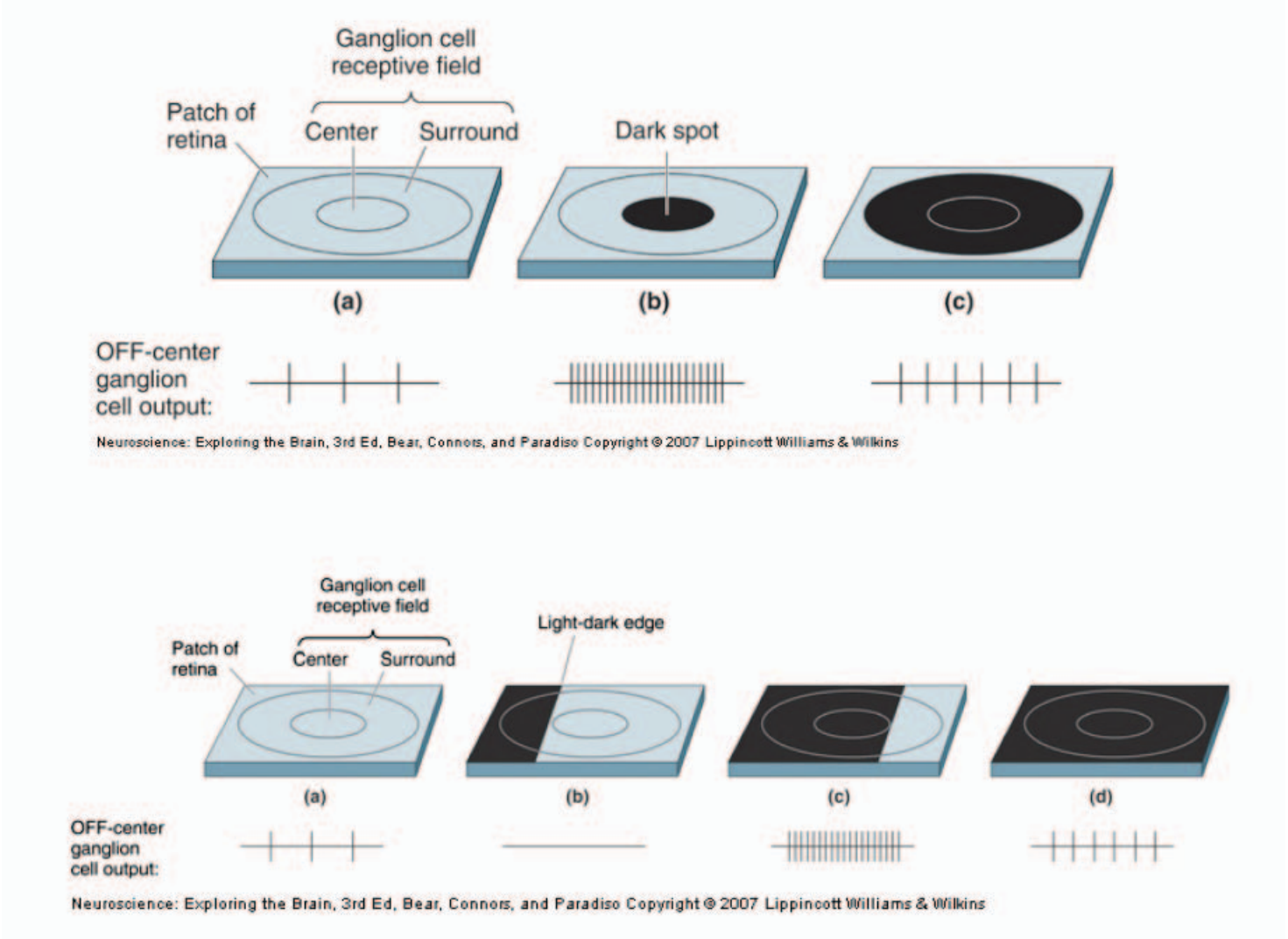

Visual information travels from retina to thalamus to cortex

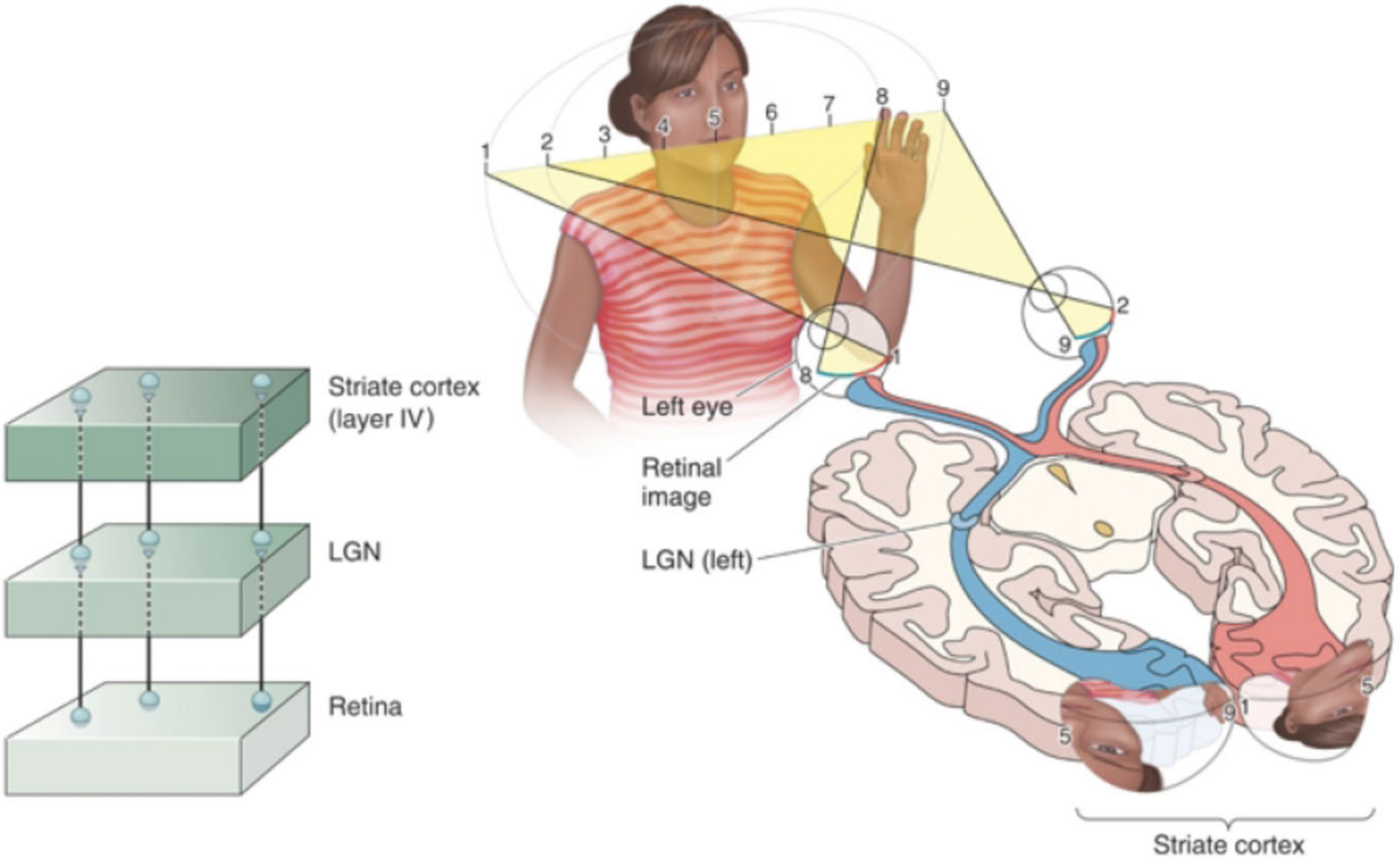

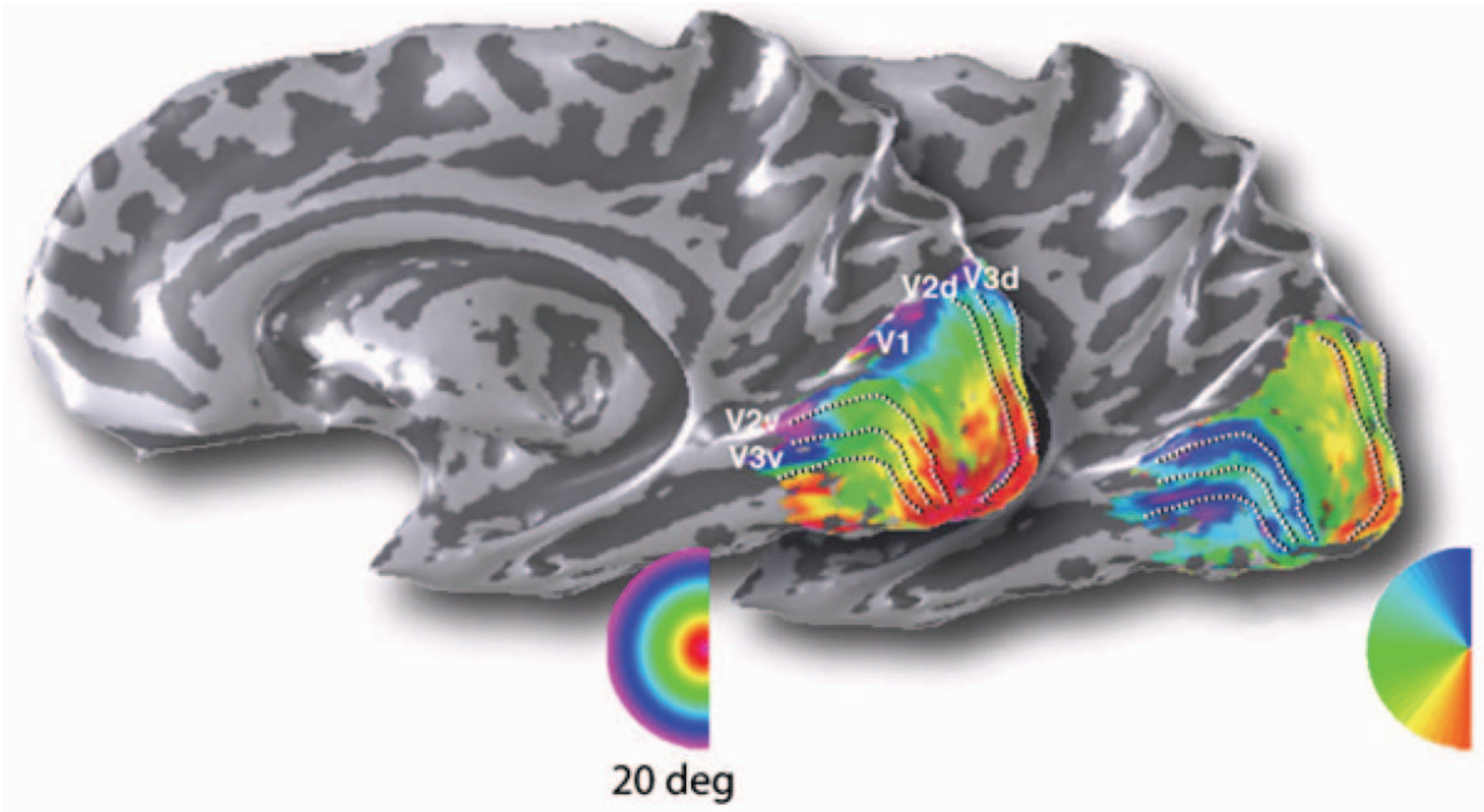

Wandell, Dumoulin, Brewer (Neuron 2007)

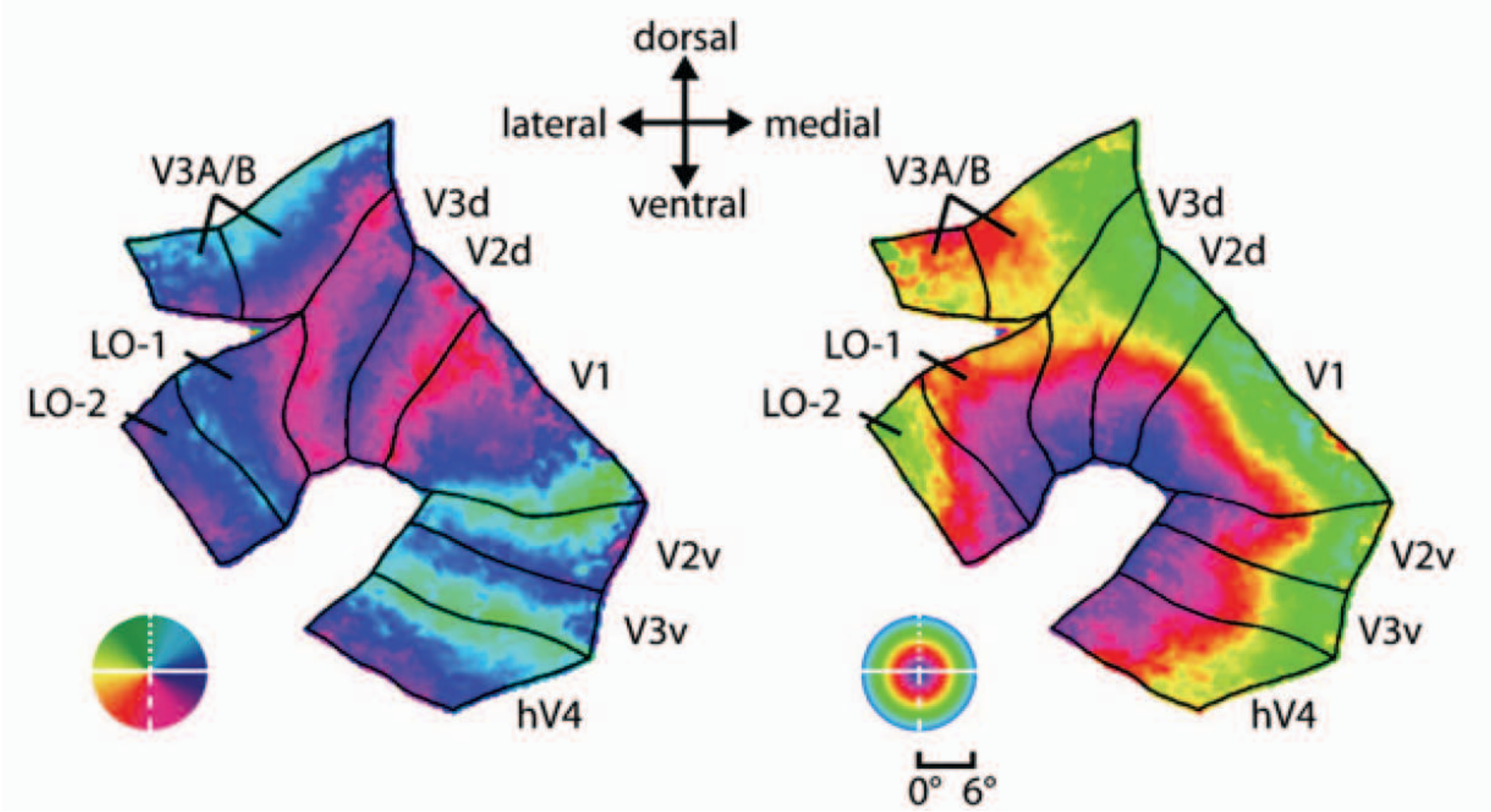

Larsson and Heeger (J Neuroscience 2006)

Cortex synthesizes orientation preference from ∇^2 receptive fields

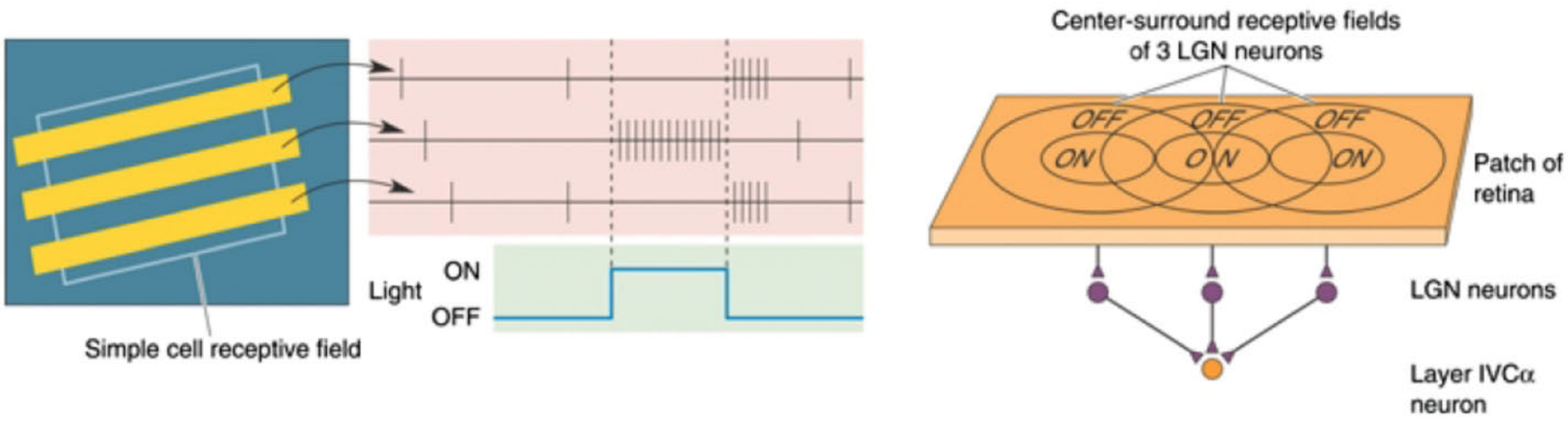

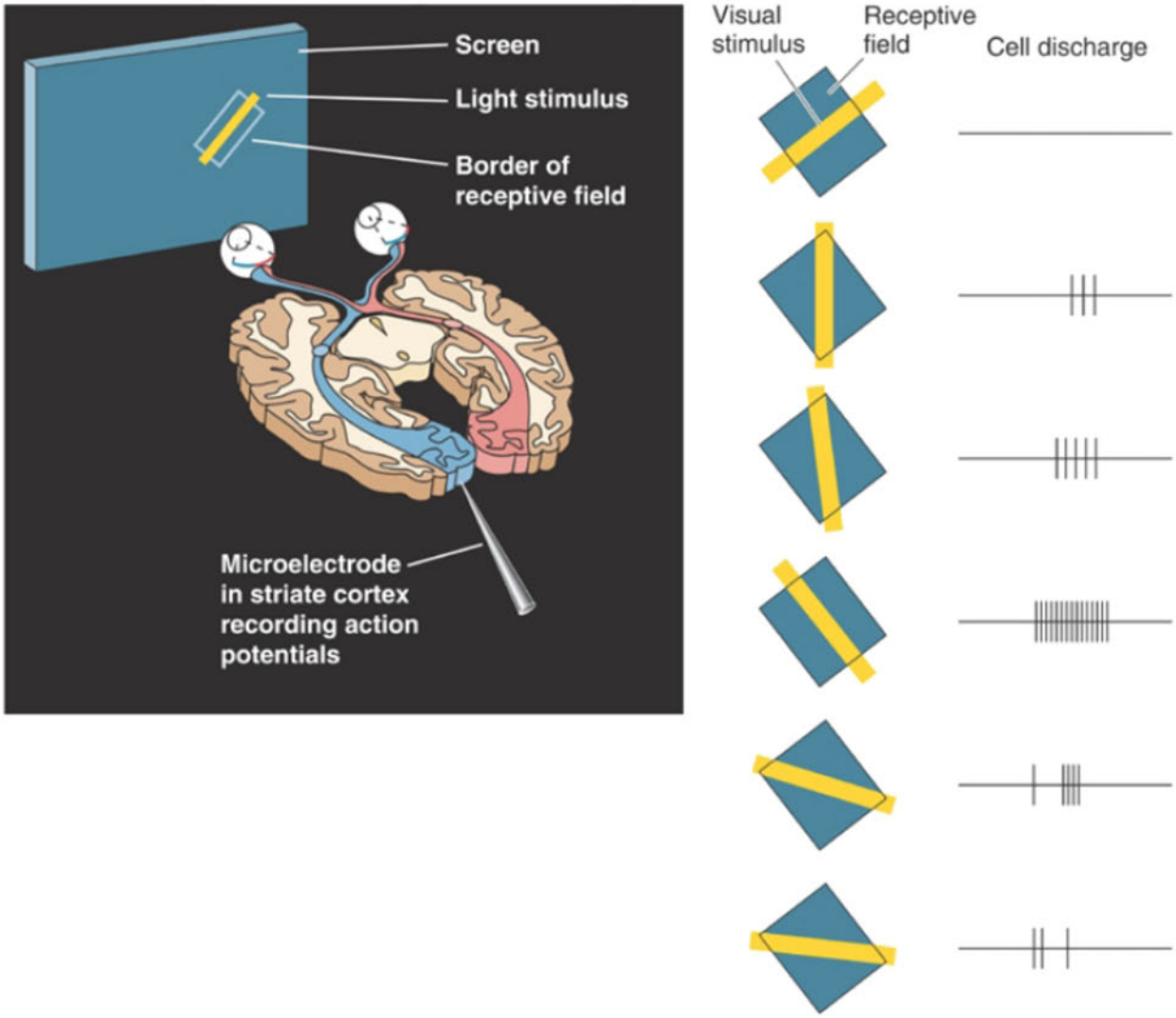

Continuous coding variables, like orientation, in primate vision, are mapped

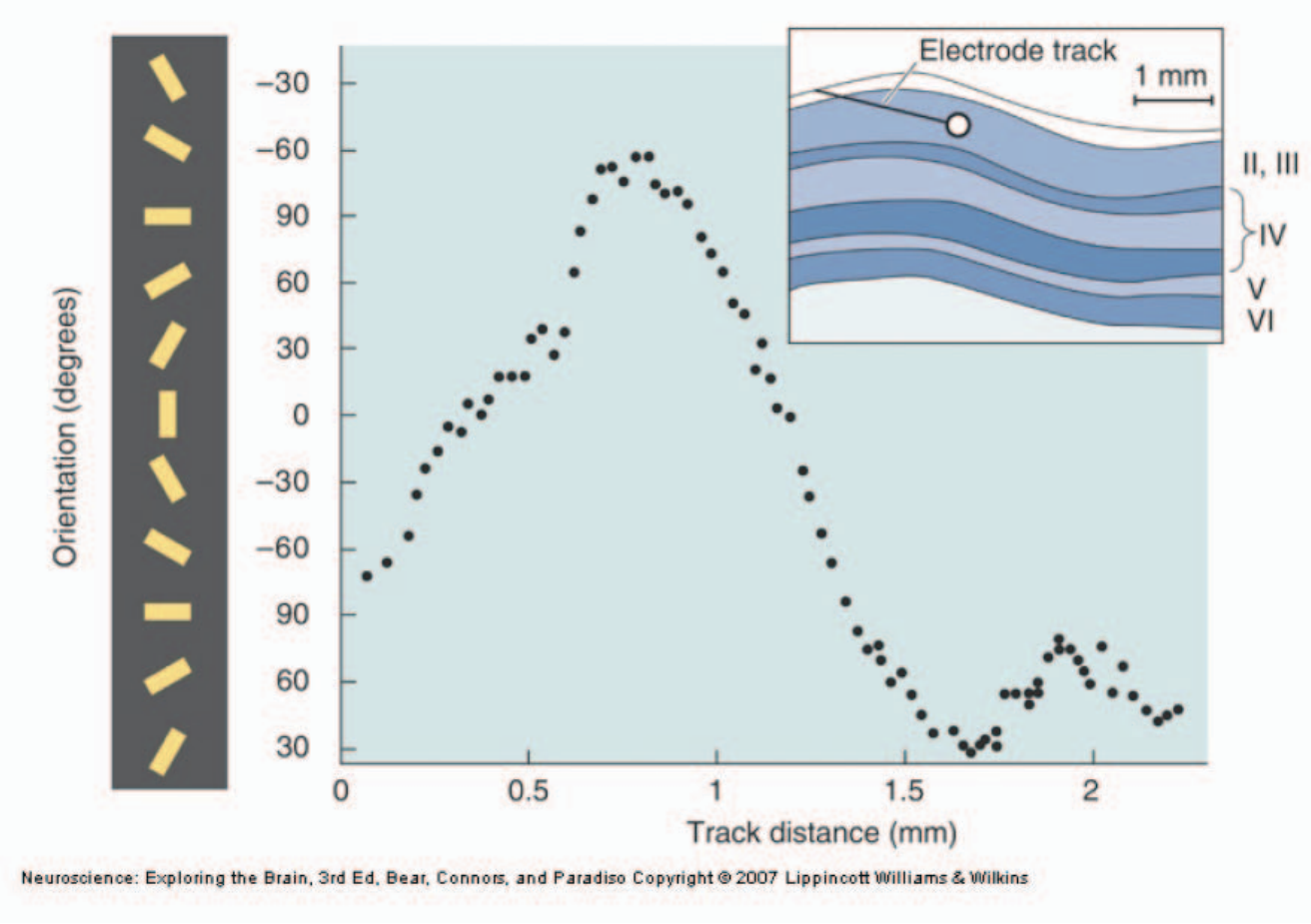

The representation of continuous coding variables can be imaged across cortex

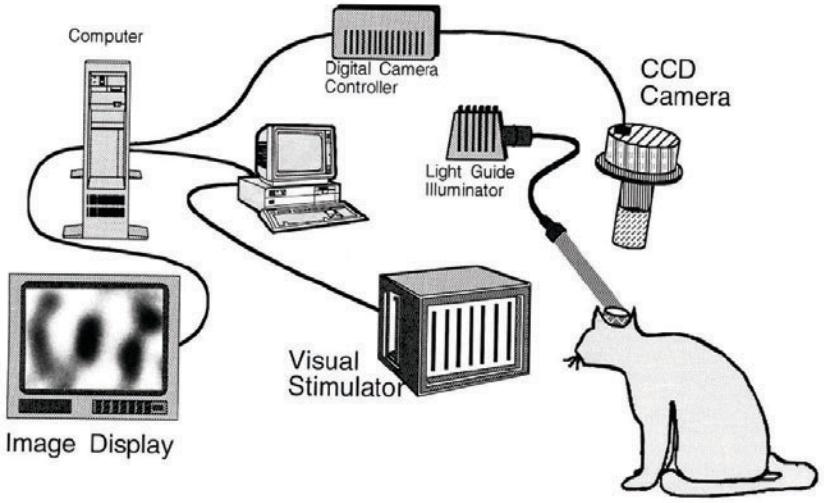

These features are mapped across visual cortex in primates and cats, as seen by intrinsic optical imaging

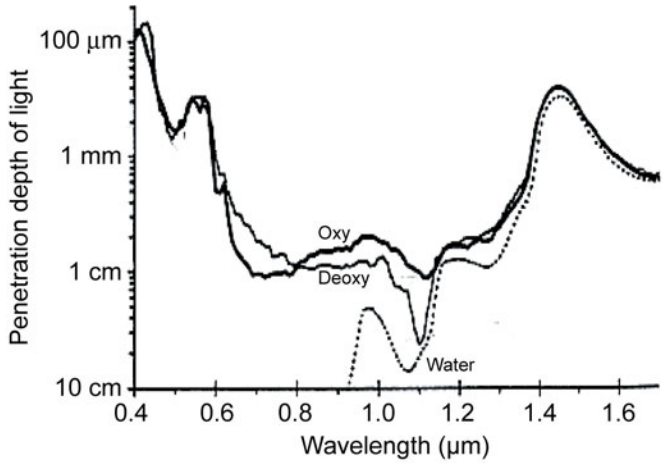

Nearby neurons have similar receptive field (but note discontinuities at spirals)

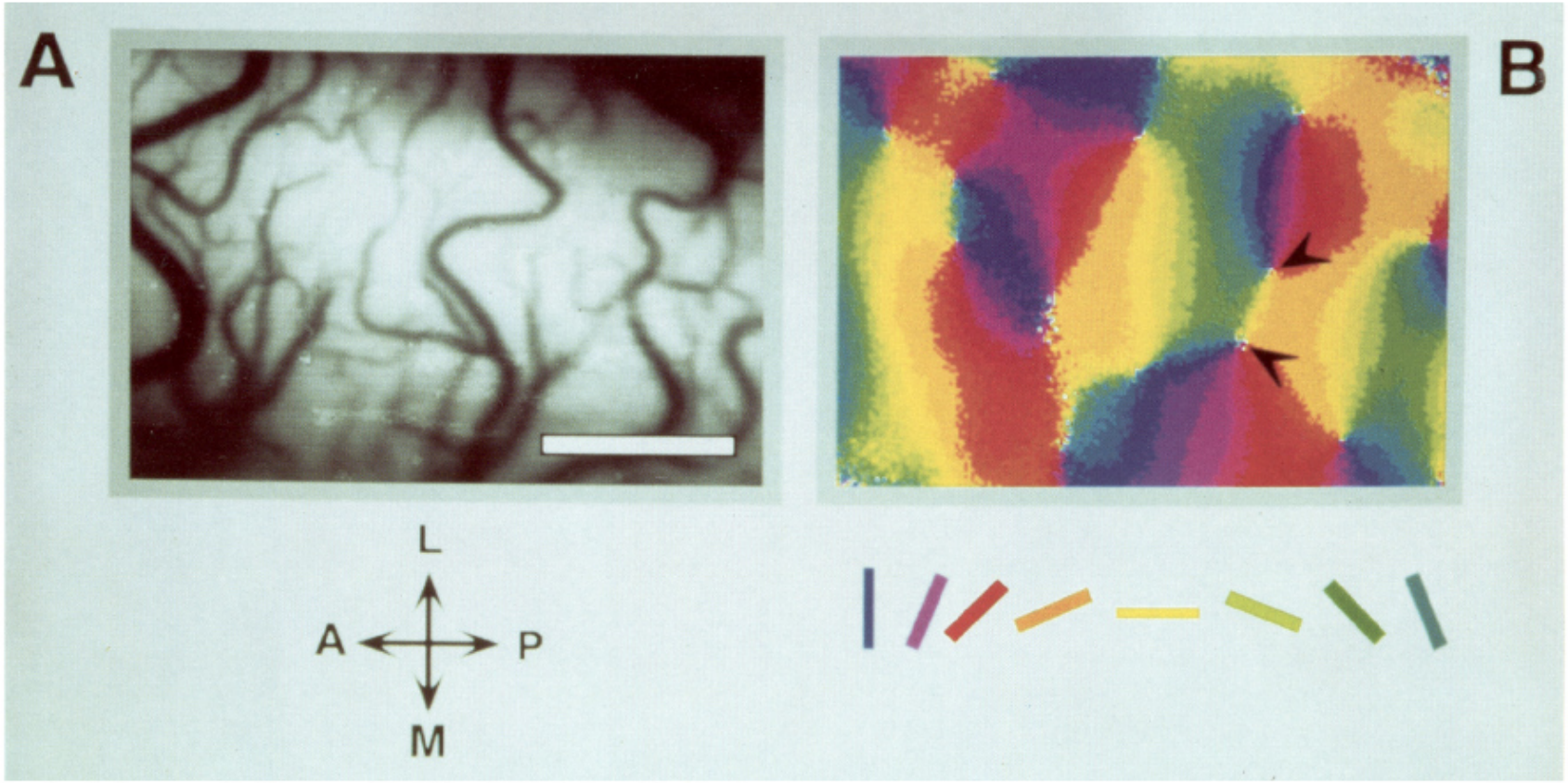

Figure 9. Angle map resulting from vectorial addition of eight single-condition iso-orientation maps. *A*, A picture of the imaged region taken in green light to emphasize the vascular pattern. *B*, Angle map showing the orientation preference for every region of the imaged cortex. For computing the local orientations we took the activity maps obtained with different orientations and added them vectorially on a pixel-by-pixel basis. The angle of the resulting vector is then color-coded according to the scheme at the bottom of the figure: *yellow* stands for sites responding best to moving gratings of horizontal orientation, regions preferring moving gratings of vertical orientation are coded in *blue*, and so on. Salient in this map are pinwheel-like structures around orientation centers (*arrowheads*). Each stimulus was averaged 48 times. No smoothing algorithms were applied. Scale bar, 1 mm.

Grinvald, Lieke, Frostig, Gilbert, Wiesel (Nature 1986)

Clarification of maps

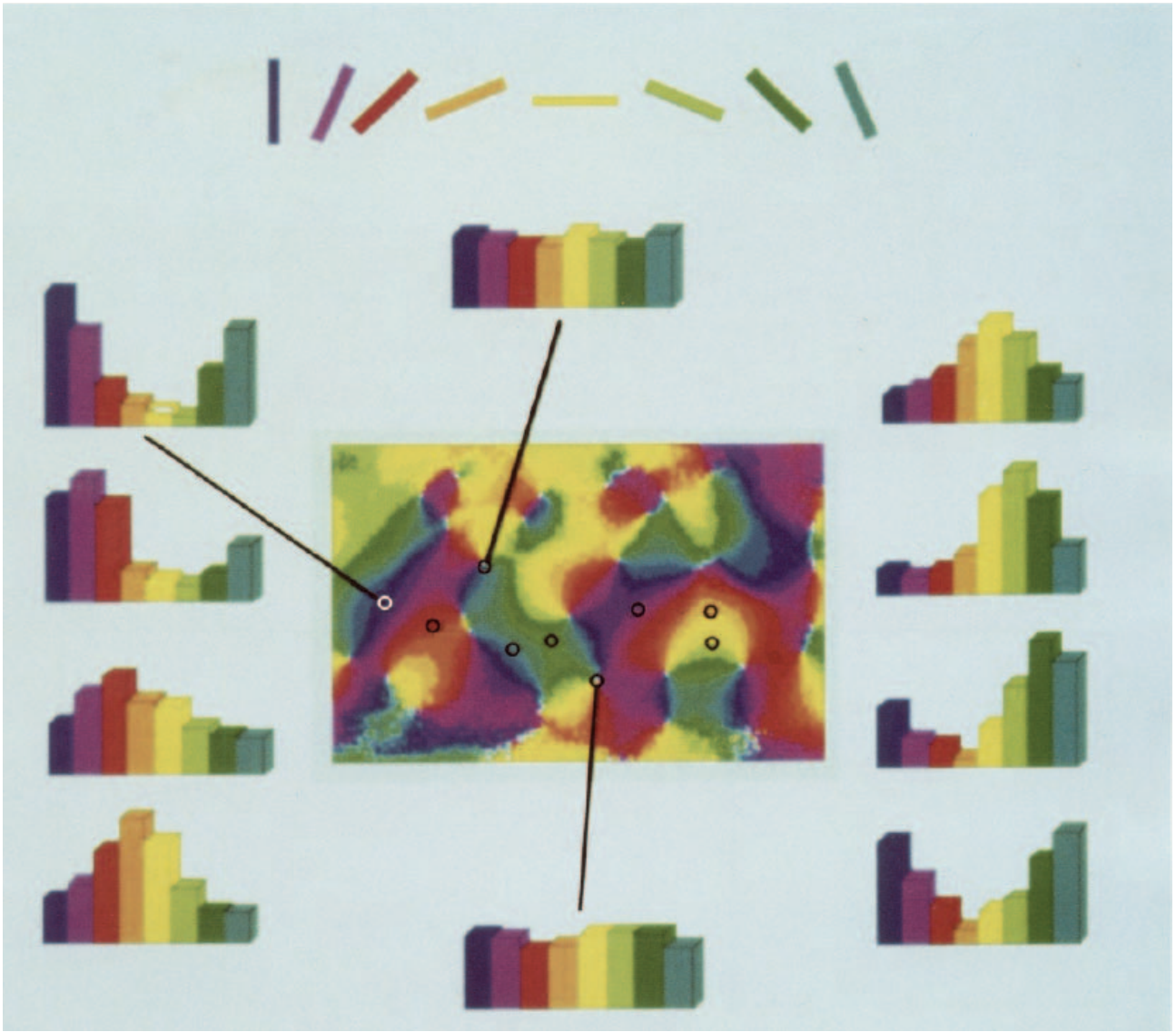

Bonhoeffer and Grinvald (J Neuroscience 1993)

Nearby neurons with similar receptive field have significant "noise" correlations

Figure 3. Correlograms obtained from two cell pairs. *A*, The cell pair had similar receptive properties: The first cell had an orientation preference of 120°, directional preference to the right and an ocular dominance group of 2, the second cell had identical orientation and direction preference and an ocular dominance group of 3. *B*, The first cell was the same cell as the first cell in *A*. The second cell had different receptive field properties: an orientation preference of 20°, upward directionality, and an ocular dominance of 5.

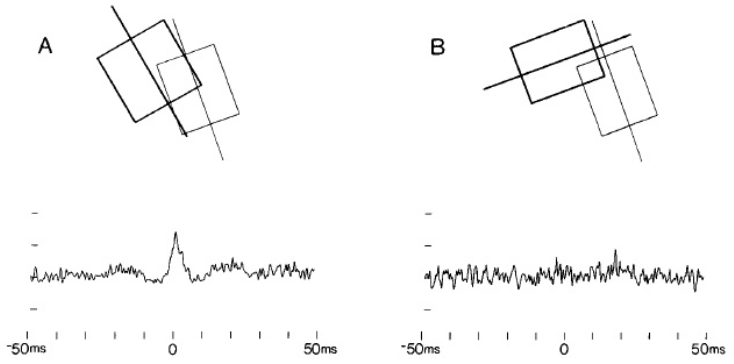

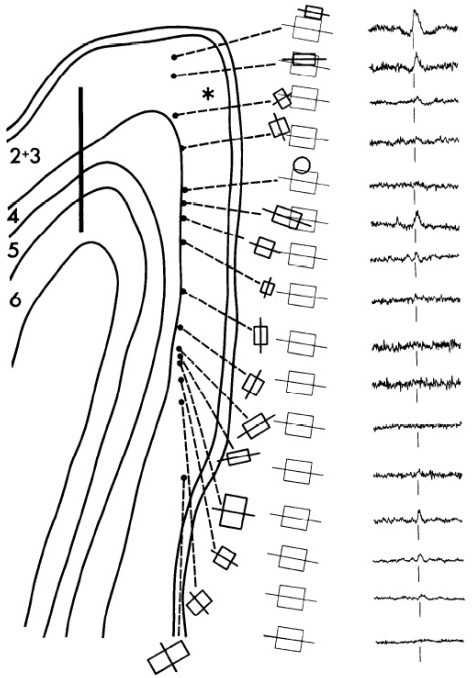

Figure 5. Medial bank penetration similar to Figure 3. Note tendency for the diminishing strength of the peaked correlograms with increases in distance between cells along the medial bank penetration and the reference cell. Also note the large difference in receptive field positions between the recording sites furthest apart.

T'so, Gilbert, Wiesel (J Neuroscience 1986)

Just a reminder - A mouse is not a monkey, and vice versa

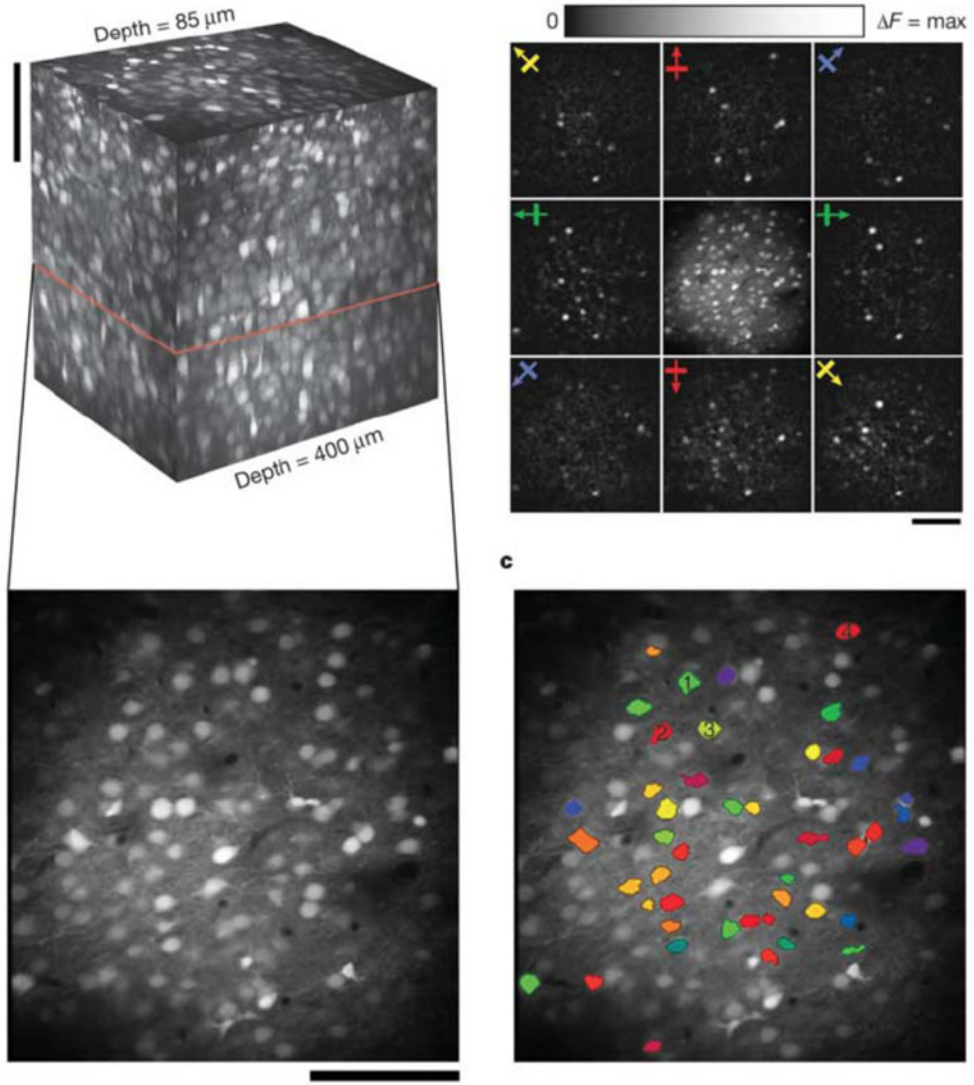

Ohki, Chung, Ch'ng, Kara, Reid (Nature 2005)

A conundrum is that the width of tuning is independent of the contrast (input strength)

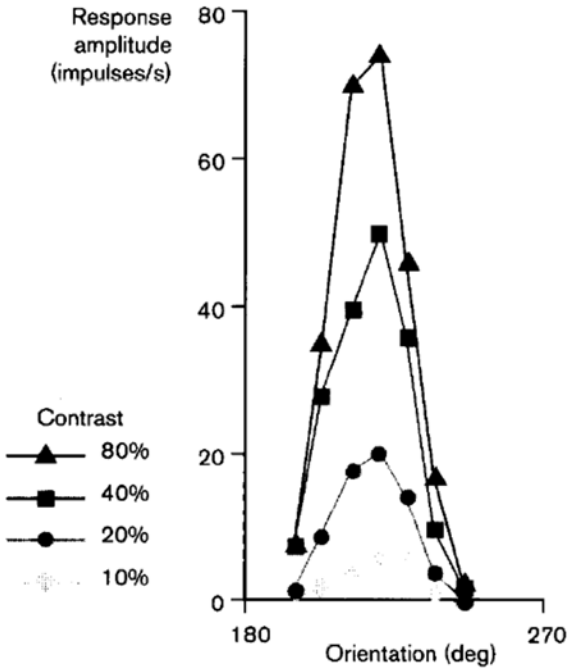

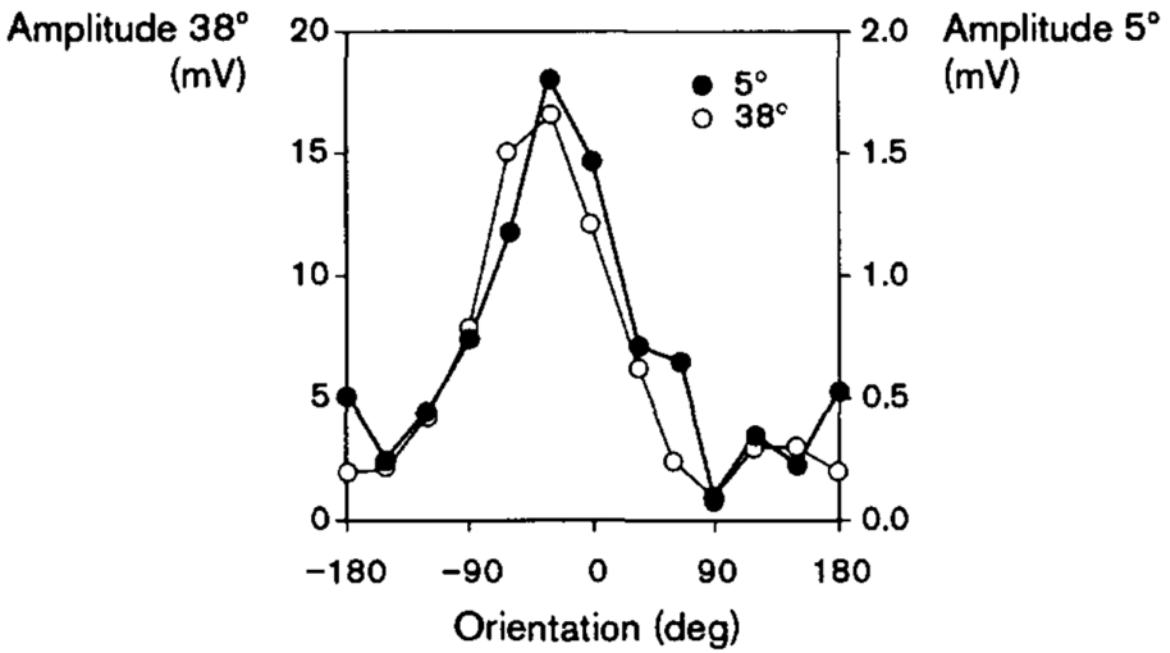

Sclar and Freeman (Experimental Brain Research 1962)

Ferster, Sooyoung, Wheat (Nature 1996)

Cortical interactions, as opposed to solely feedforward features, define the tuning width

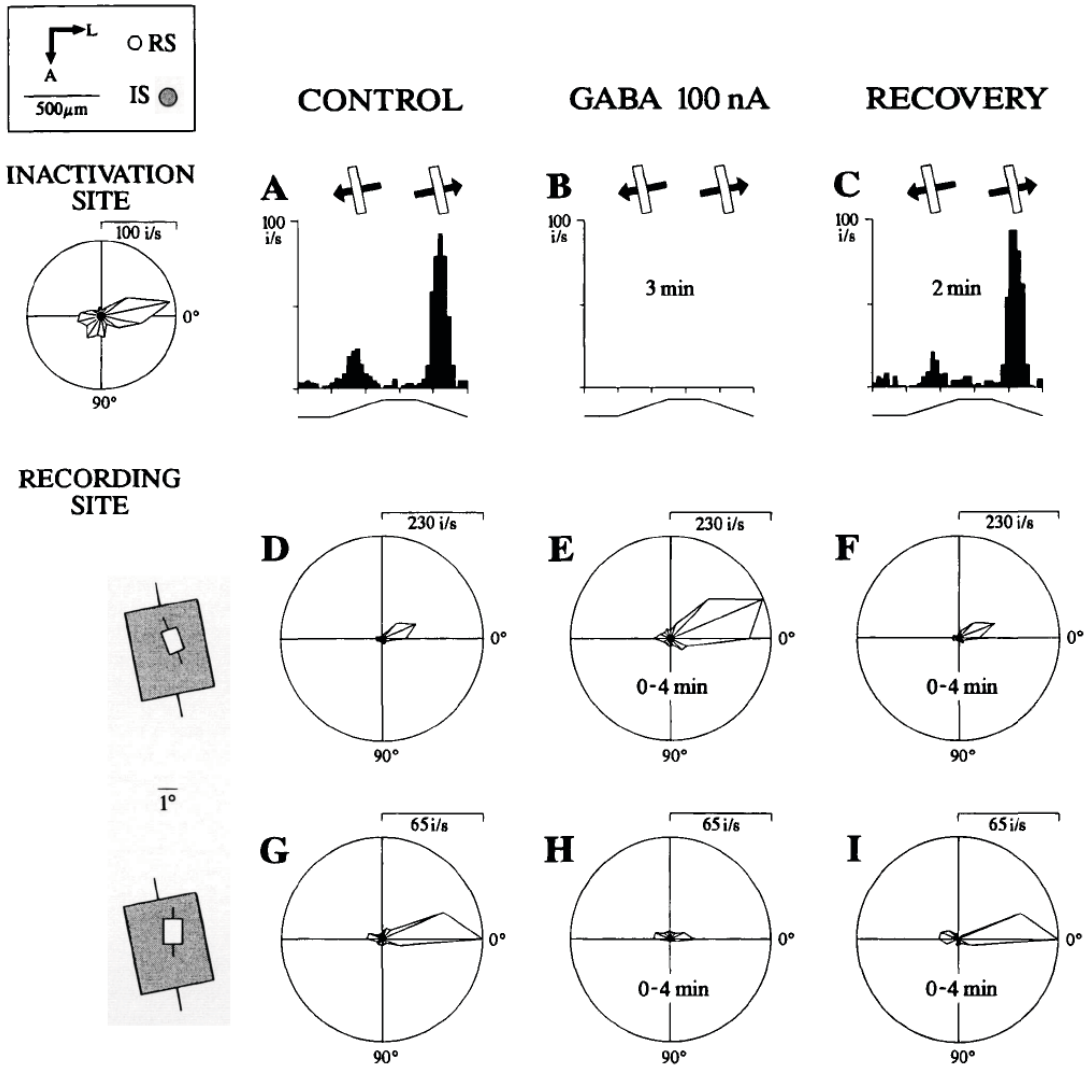

Crook, Kisvarday, Eysel (Visual Neuroscience 1997)

Beyond vision, normalization of input signals is seen in other systems, e.g., the coding of touch by the vibrissa system of rodents

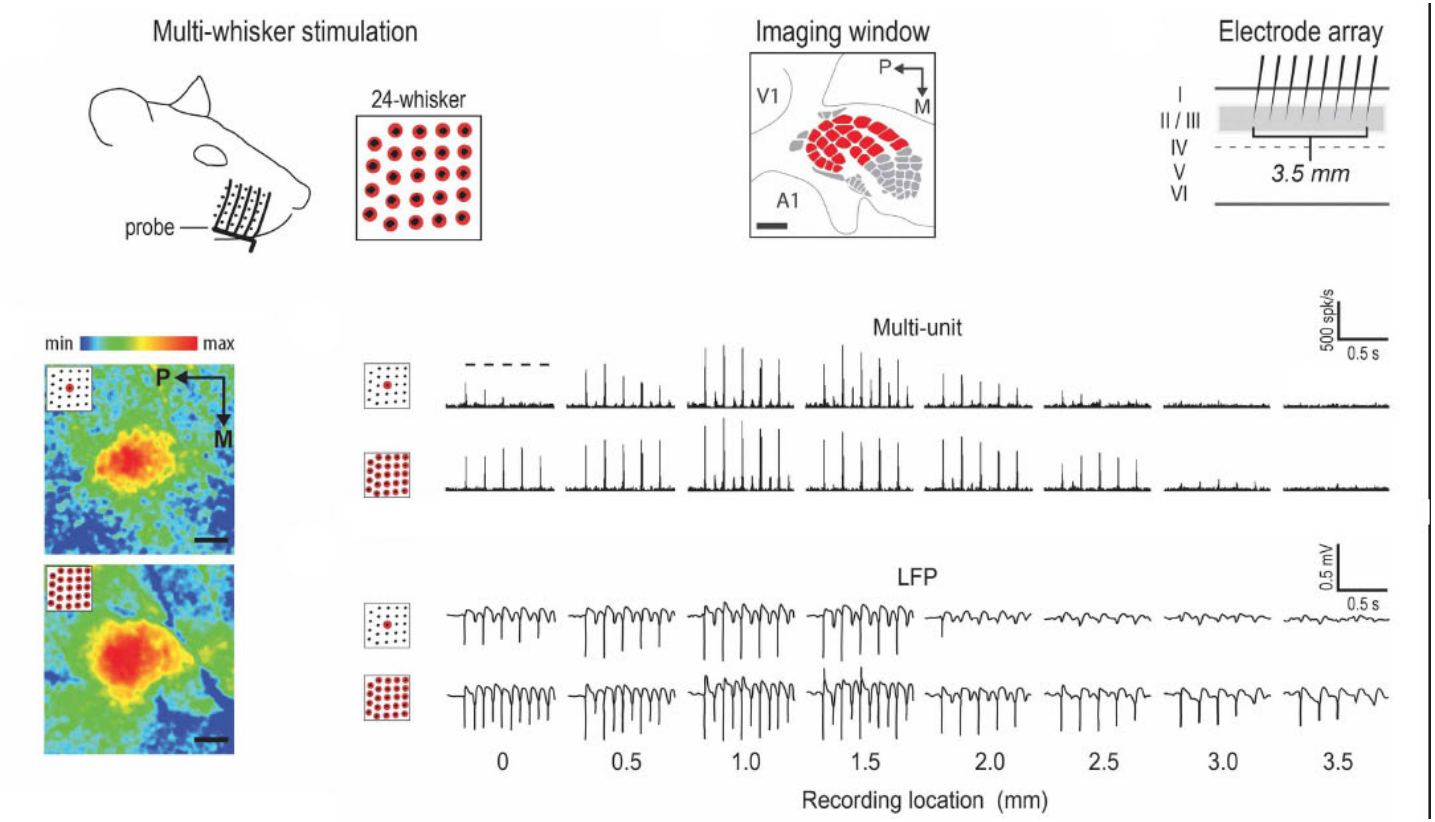

Chen-Bee, Zhou, Jacobs, Lim, Frostig (Frontiers of Neural Circuits 2012)

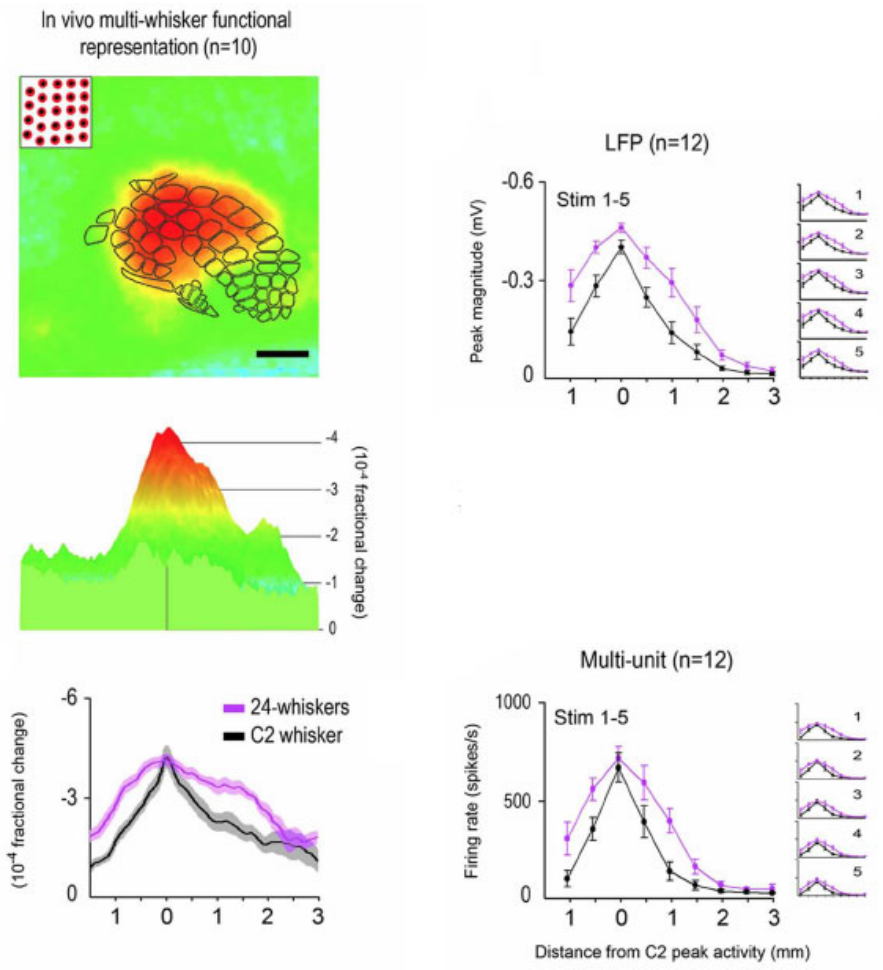

Chen-Bee, Zhou, Jacobs, Lim, Frostig (Frontiers of Neural Circuits 2012)

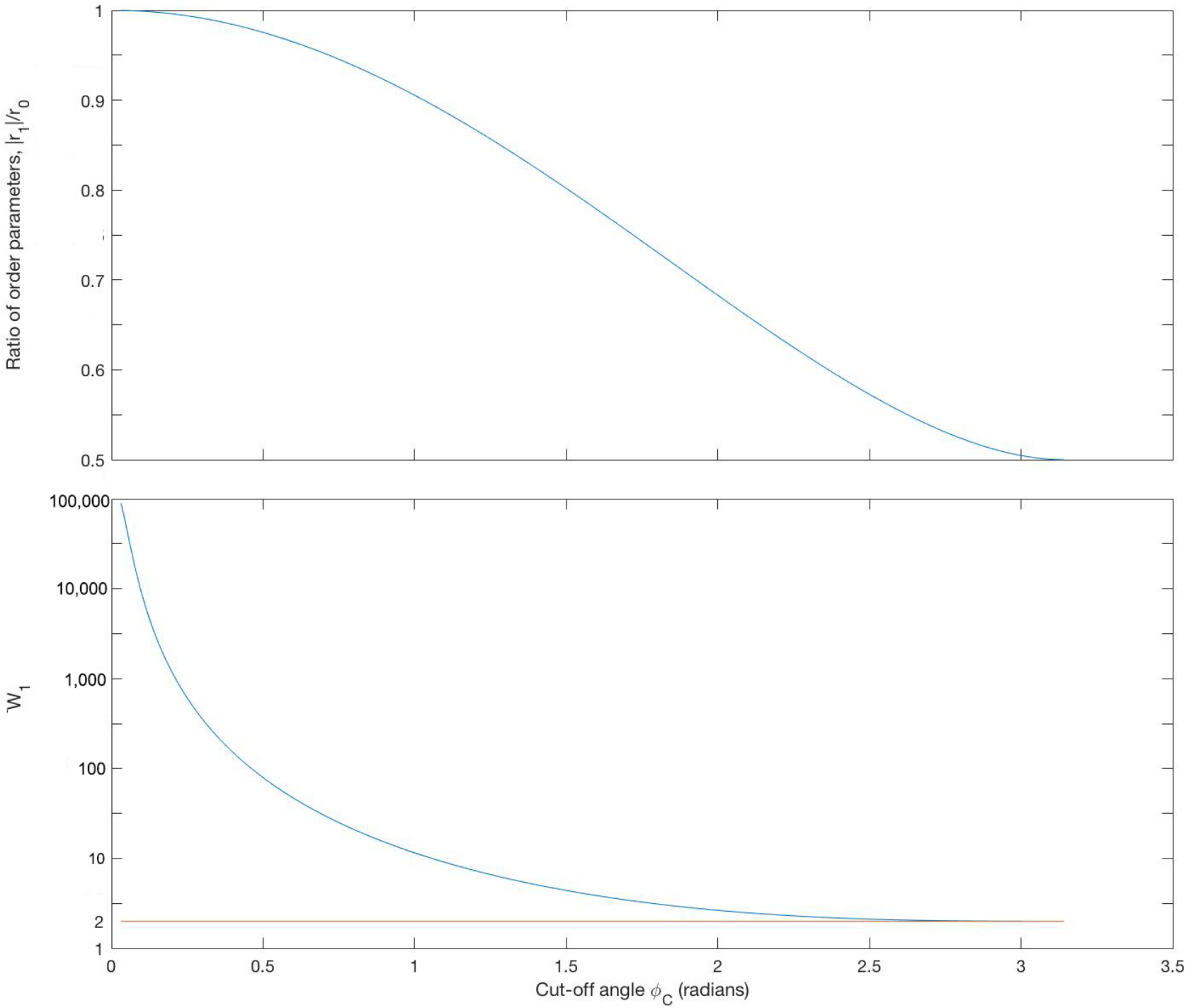
Ratio of order parameters, $|r_1|/r_0$
1
0.9
0.8
0.7
0.6
0.5
W_1
100,000
10,000
1,000
100
10
2
1
0
0.5
1
1.5
2
2.5
3
3.5
Cut-off angle ϕ_C (radians)

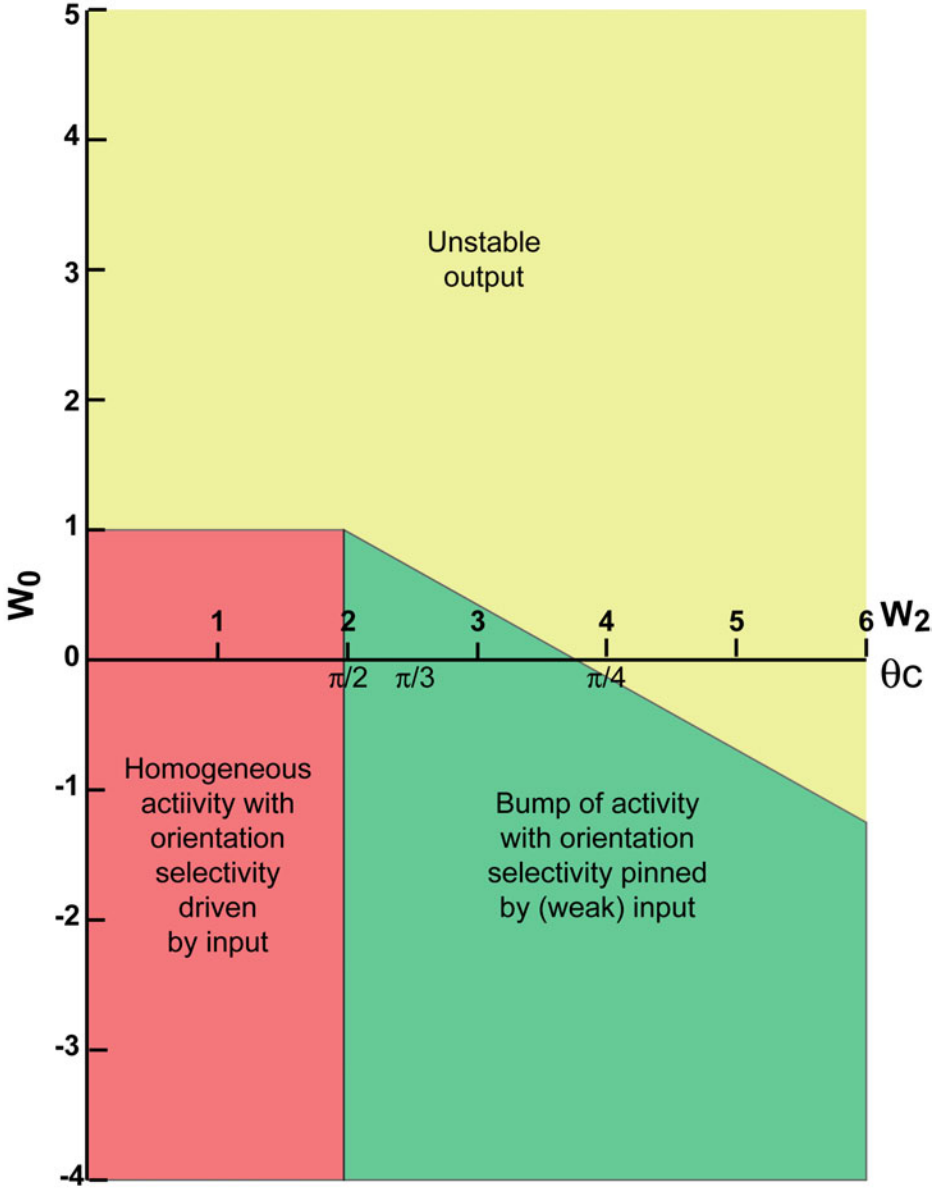
5
4
3
2
1
0
-1
-2
-3
-4
W0
Unstable
output
1
2
3
4
5
6
W2
π/2
π/3
π/4
θc
Homogeneous
actiivity with
orientation
selectivity
driven
by input
Bump of activity
with orientation
selectivity pinned
by (weak) input

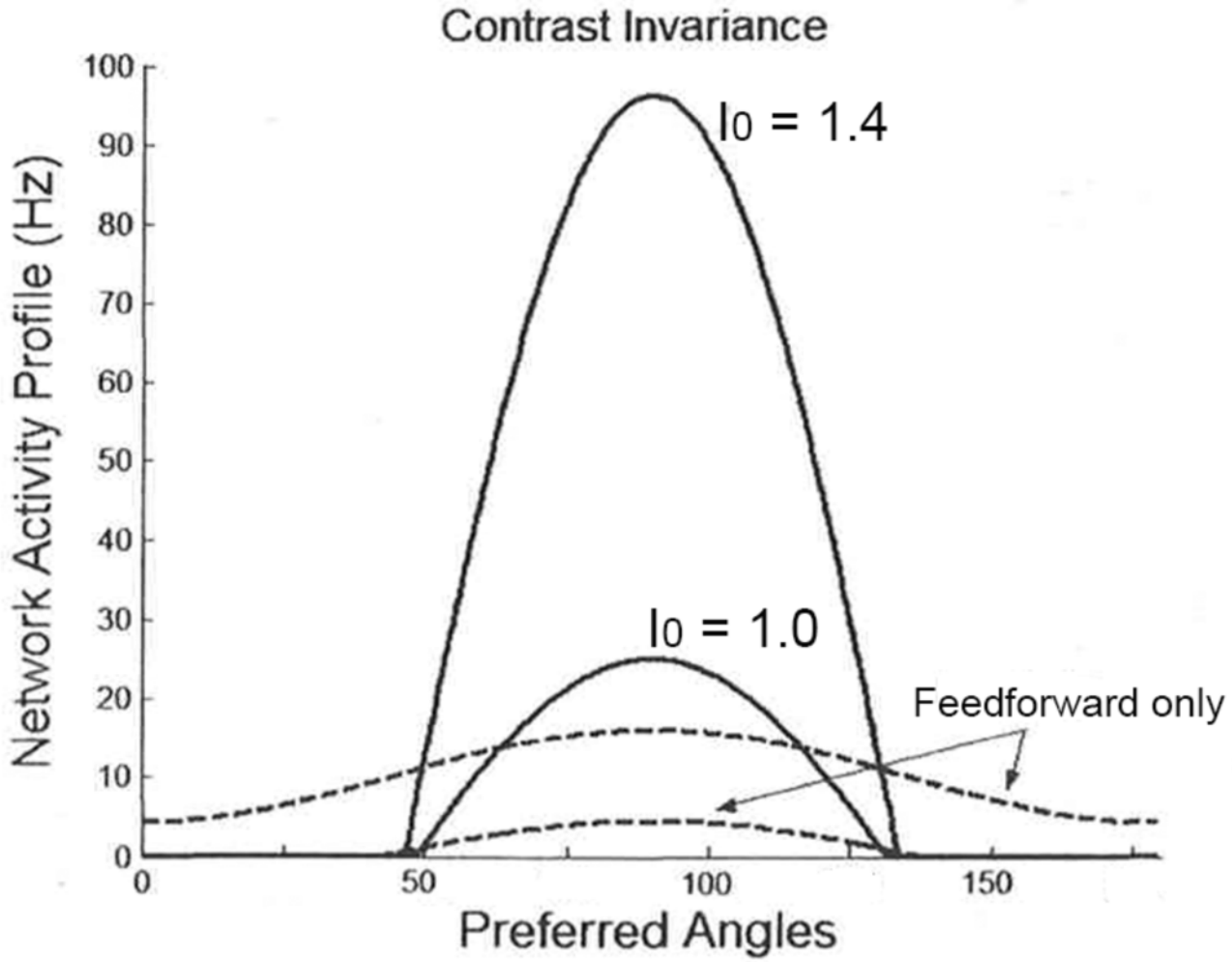

$W_0 = -0.4$ and $W_2 = 4.0$

$\varepsilon = 0.09$

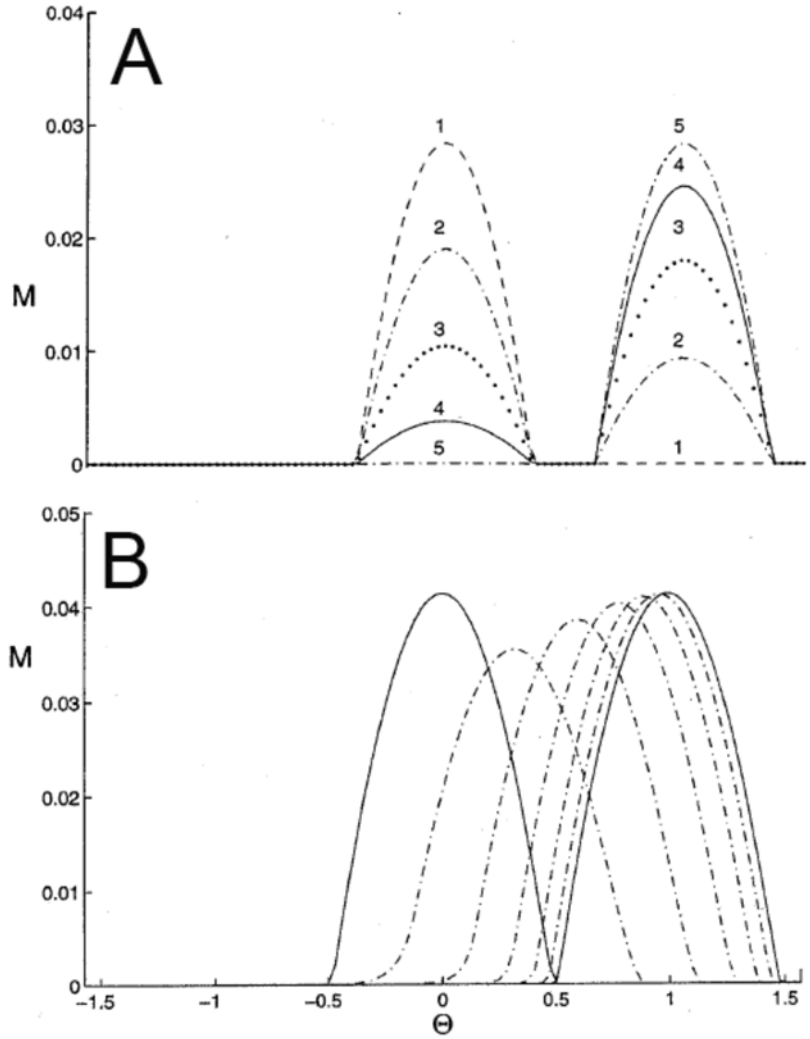

Figure 13.9
Evolution of the neuronal activity in response to a change in the stimulus orientation from an initial value $\theta_1 = 0^0$ to $\Theta_2 = 60^0$. The change occurs at $t = 0$. (A) Afferent mechanism with uniform inhibition. Parameters: $J_0 = -15.5$, $C = 1.1$, $\varepsilon = 0.5$. Times (units of τ_0): 0, 0.5, 1, 2, 6 (lines 1–5, respectively). (B) Virtual rotation in the marginal phase. The activity profile is moving toward θ_2. Parameters: $J_0 = -17.2$, $J_2 = 11.2$, $\varepsilon = 0.05$, $C = 2$. Times (left to right): 0 to $35\tau_0$ each $5\tau_0$.

Bumps of activity in the heading direction system in rodent thalamus

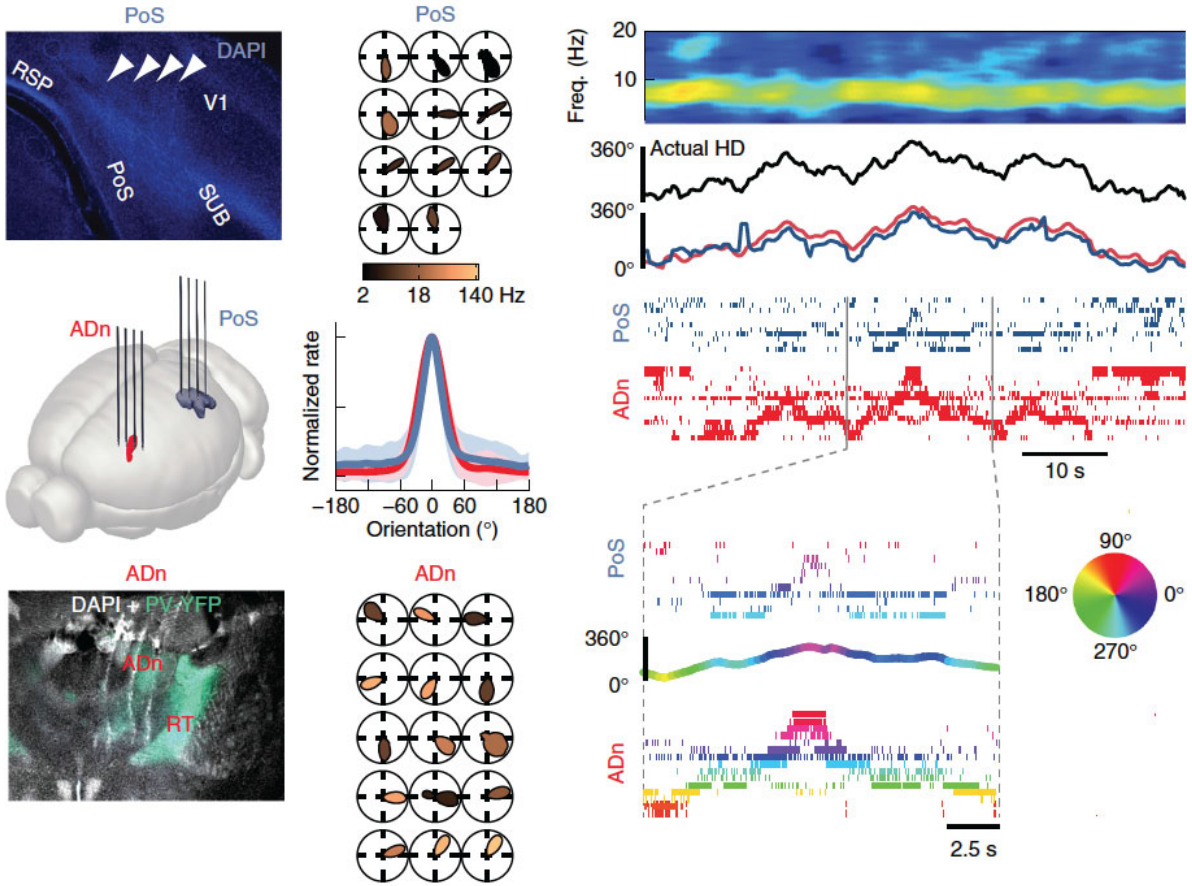

Internally organized mechanisms of the head direction sense
Nature Neuroscience 2015
Adrien Peyrache, Marie M Lacroix, Peter C Petersen & György Buzsáki

Bumps of activity in the landmark heading system in the fly ellipsoid body of the central complex thalamus

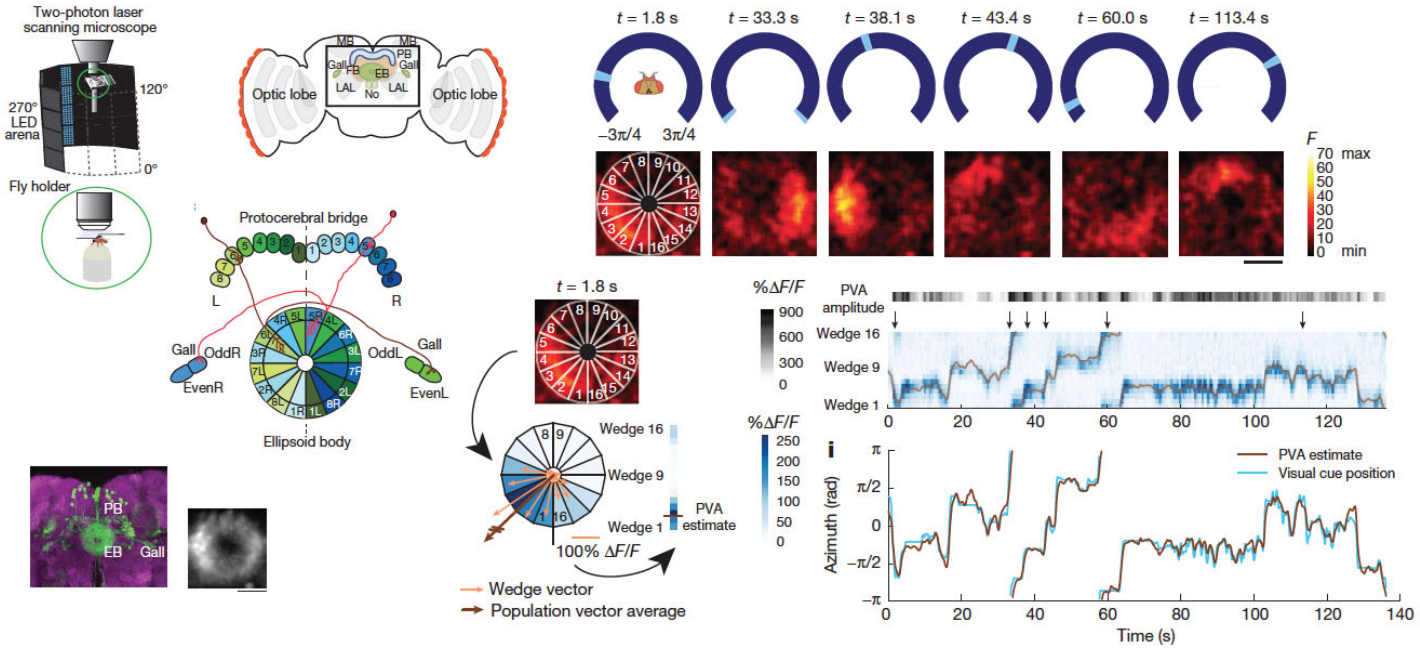

Neural dynamics for landmark orientation and angular path integration
Nature
Johannes D. Seelig & Vivek Jayaraman

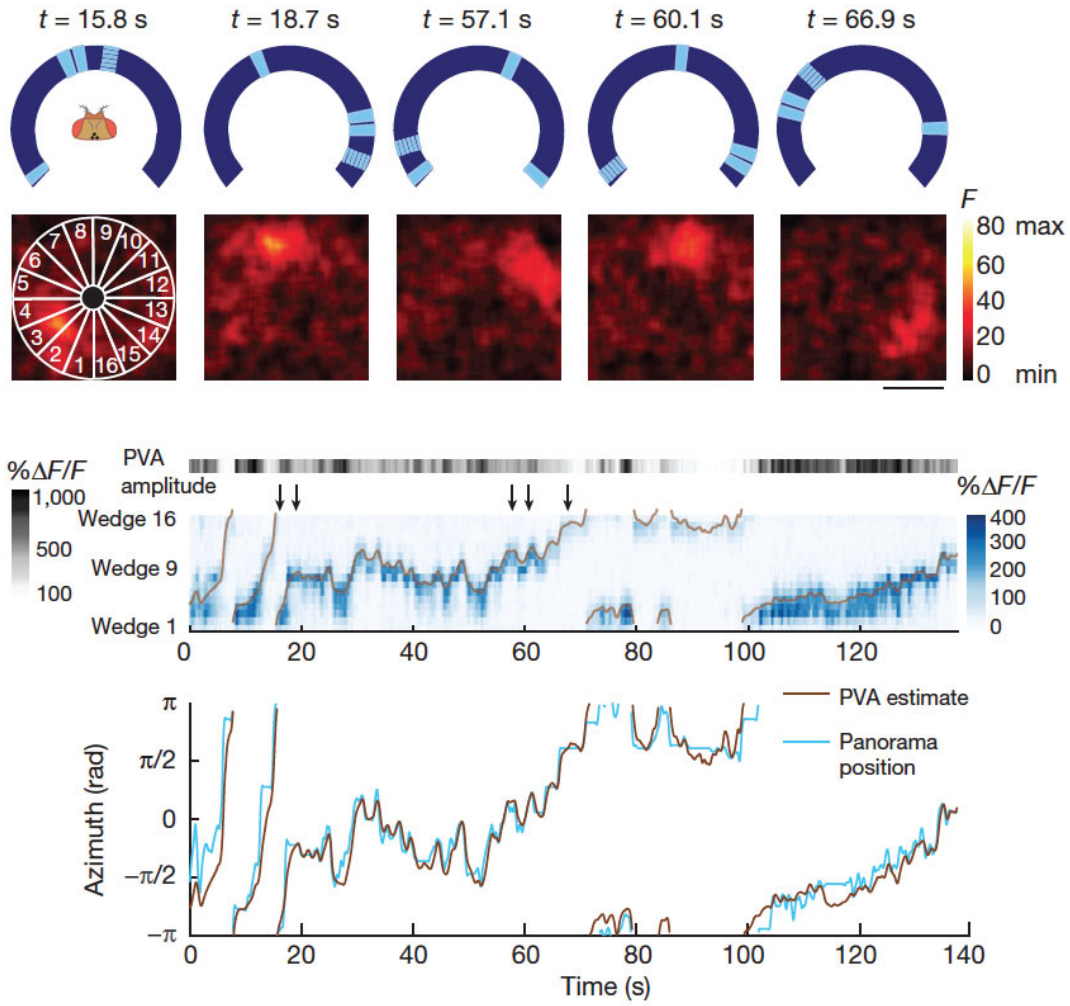

Neural dynamics for landmark orientation and angular path integration
Nature
Johannes D. Seelig & Vivek Jayaraman

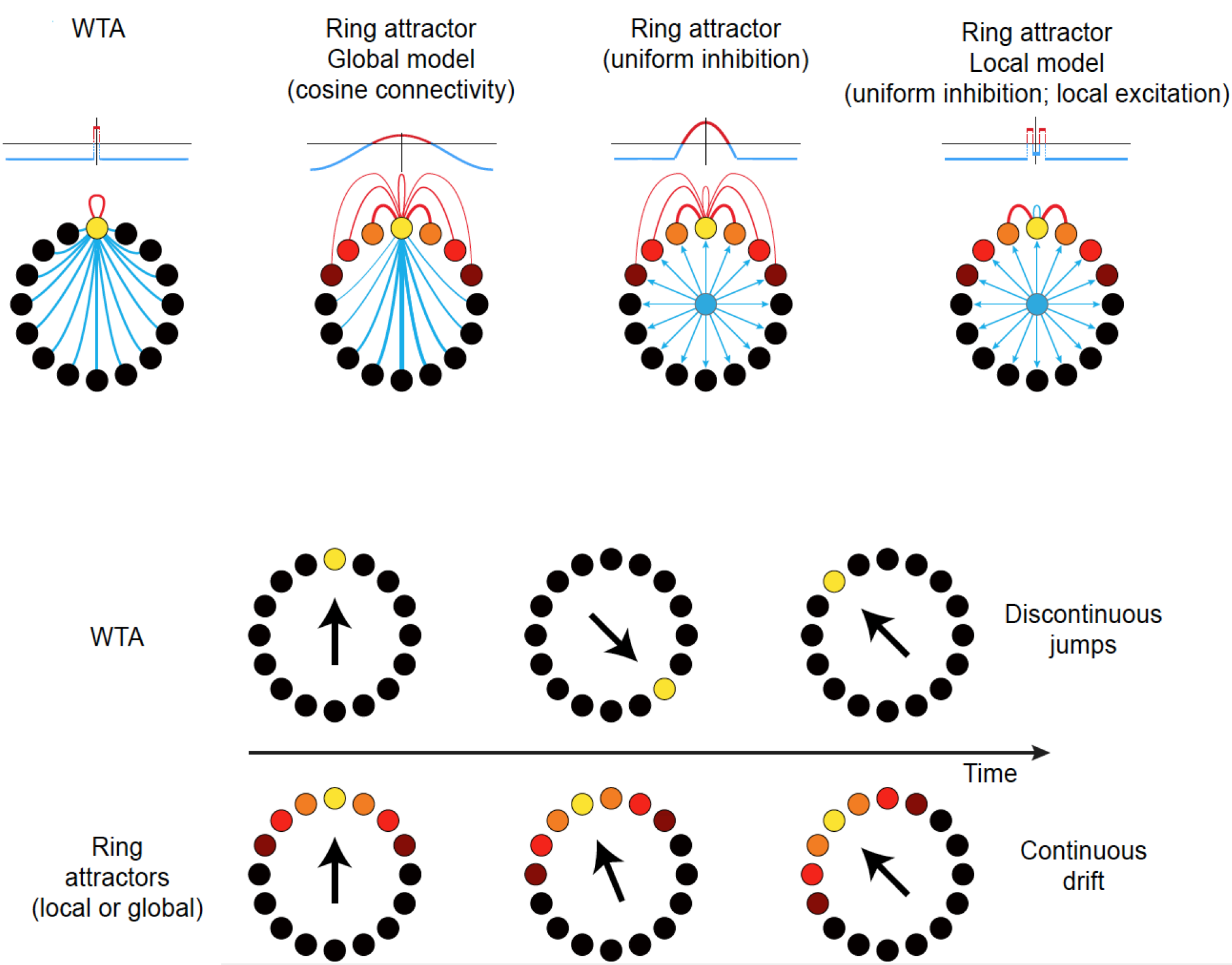
WTA
Ring attractor
Global model
(cosine connectivity)
Ring attractor
(uniform inhibition)
Ring attractor
Local model
(uniform inhibition; local excitation)
WTA
Discontinuous
jumps
Time
Ring
attractors
(local or global)
Continuous
drift